

# The geotechnical evaluation of sandstone–claystone alternations based on geological strength index

Ahmet Özbek · Murat Gül

Received: 21 February 2014 / Accepted: 4 July 2014 / Published online: 5 August 2014  
© Saudi Society for Geosciences 2014

**Abstract** The aim of this study is to classify heterogeneous deep-sea sediments (including sandstone and claystone) according to the geological strength index (GSI). Forty-nine locations have been selected from excavated Miocene deep-sea clastic sediments bearing slopes from the Kahramanmaraş Basin (SE Turkey). Six rock classes are determined based on sandstone/claystone ratios (S/C). Those rock classes and their percentages are ‘B’ class of 39 % ( $1 < S/C \leq 10$ ); ‘D’ class—20 % ( $1/3 \leq S/C < 1$ ); ‘C’ class—16 % ( $S/C \geq 1/1$ ); ‘E’ class—14 % ( $1/10 \leq S/C < 1/3$ ); and rest 11 % formed by ‘F’ class (tectonically deformed), ‘G’ class ( $S/C < 1/10$ ), and ‘A’ class ( $S/C > 10$ ). Four different groups of rock are separated according to GSI based on rock classes and discontinuity surface conditions (‘A–B’ class,  $GSI > 40$ ; ‘C’ class,  $35 \leq GSI \leq 40$ ; ‘D–E’ class,  $25 \leq GSI < 35$ ; ‘F–G’ class,  $GSI < 25$ ). The lower values of the Mohr–Coulomb and strength parameters of rock mass (cohesion- $c$ , internal friction angle- $\phi$ , and deformation modulus- $E_m$ ) are observed in the ‘E–D’ classes due to high clay content, while higher values in the ‘A–B’ classes due to high sand content.

**Keywords** GSI · Geotechnical evaluation · Heterogeneous rock masses · Sandstone–claystone

---

A. Özbek (✉)  
Department of Geological Engineering, Kahramanmaraş Sutcu Imam University, 46100, Avsar Campus, Kahramanmaraş, Turkey  
e-mail: ozbekaderen@gmail.com

A. Özbek  
e-mail: ozbeka@ksu.edu.tr

M. Gül  
Department of Geological Engineering, Mugla Sıtkı Kocman University, 48000, Kotekli Campus, Mugla, Turkey

## Introduction

Determinations of the geotechnical characteristics and rock classes of the heterogeneous rocks (such as schist and gneiss of metamorphic rocks and conglomerate–sandstone–claystone alternations of sedimentary rocks) have been one of the most important issues of the rock mechanics. The heterogeneous characters of rock may also source from the internal fractural properties including discontinuities, pores, and grains (Ma et al. 2013; Moomivand 2014). These properties affect the stress and strain behaviors and geomechanical characteristics of rock, which are fundamental elements of rock classifications (Şen 2014). The main rock classification systems (RQD, RMR, and Q) are prepared based on the uniaxial compressive strength, discontinuity properties, stress parameters, and groundwater conditions. The lithological differences of rock masses are not considered in these classifications. Hoek and Brown (1980) suggested that deformation properties and heterogeneity of rock must be taken into consideration during the rock mass classification. So, Hoek et al. (1995), and Hoek and Brown (1997) introduced the concept of the geological strength index (GSI) for the classification of heterogeneous rock masses. The Hoek and Brown parameters and GSI can be used in various engineering geological applications such as dam (Agan 2014; Alemdag 2014) and tunnel (Amit Verma and Singh 2010).

The Miocene-aged deep-sea sediments crop out in the north of the Kahramanmaraş province (SE Turkey). The sedimentation process (such as channel formation, channel-lobe transition, lobe-basin plain transition, energy of current, sediment type, sediment entry points, etc.), distance from basin margin, and irregularity of basement topography led to the deposition of conglomerate, sandstone, and claystone alternation with varying ratios (Önalın 1988; Derman 1999; Gül 2004). Several dams and small reservoirs (under construction)

are located in the north of Kahramanmaraş. The highways supplying the connection between the Kahramanmaraş province and other city centers have been also excavated in the Miocene geologic units (Fig. 1). The slope, road, foundation excavations, and dam constructions in this area have been suffering from instability problems due to the heterogeneity of the rocks. The examples of these type deep-sea sediments

with various ages can be seen in different regions of Turkey and in the world (Walker 1978; Gül et al. 2012a). Even though there are many publications on occurrences, distribution, and reservoir characteristics of the deep-sea sediments due to their potential oil and natural gas contents (Walker 1978; Bouma 2004; Gül et al. 2012a and references therein), geotechnical characteristics studies are limited (only project reports).

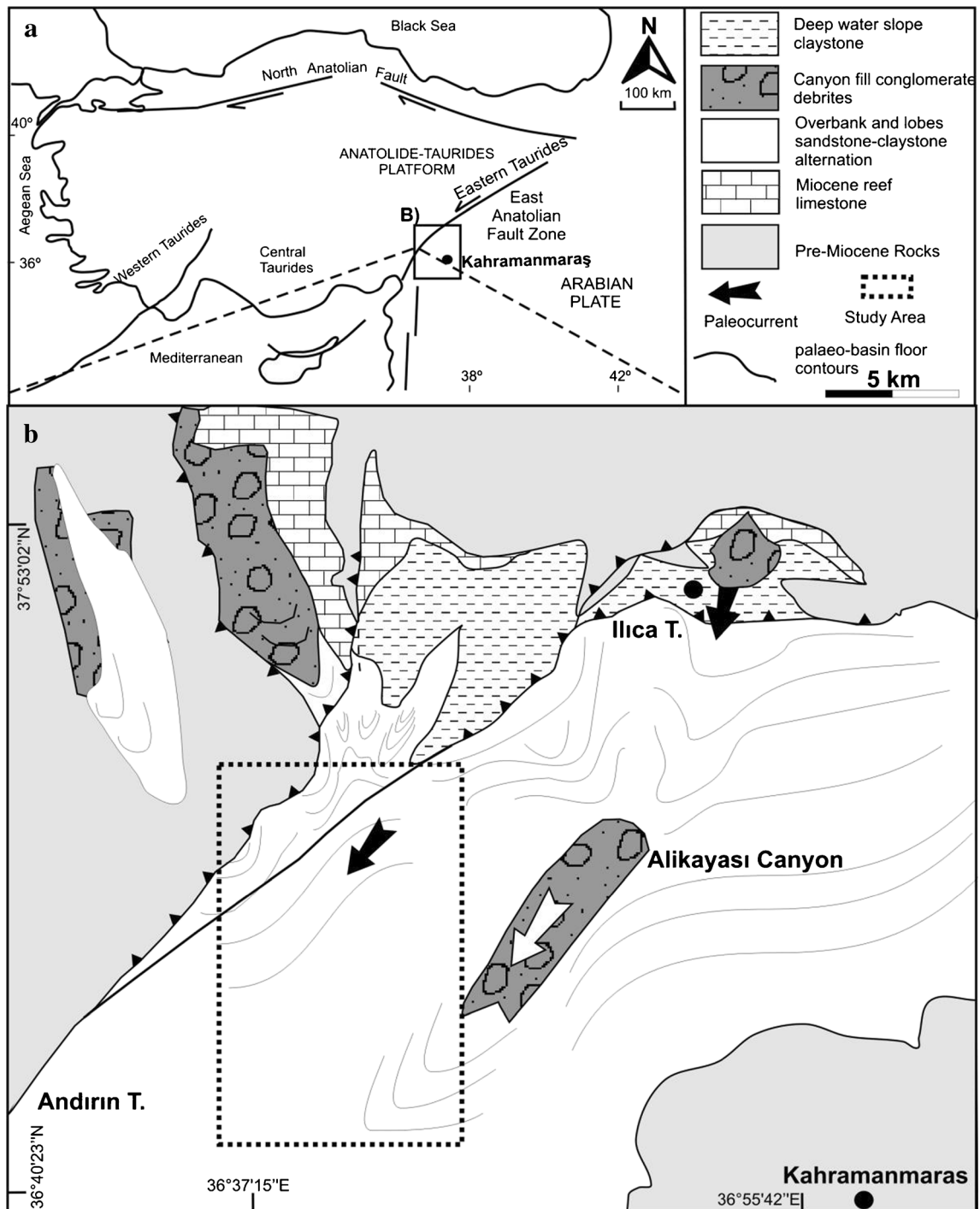


**Fig. 1** a The study area is located in southeastern Turkey, close to the active East Anatolian Fault Zone (Kissel et al. 2003). b Older rock and Miocene sediment distribution in the Kahramanmaraş Basin (modified after, Derman 1999; Gül et al. 2012a)

The aim of this study is to determine the geotechnical characteristics and classification of heterogeneous deep-sea sediments (N Kahramanmaraş) based on the Hoek–Brown failure criteria (used to GSI and S/C ratio). Marinos and Hoek (2001) proposed eight different rock classes taking into account field observations and sandstone and finer-grained sediment rates. These classes are used for determining the value of GSI of heterogeneous rock masses such as flysch. This classification is prepared based on qualitative properties, which vary over a wide range. Budetta and Nappi (2011) proposed an additional quantitative classification using the S/C ratio for the San Mauro Formation in Italy.

In this study, six different quantitative rock classes are proposed based on field observations in the Kahramanmaraş terrain. The discontinuity characteristics, composition, and structural properties of the heterogeneous deep-sea sediments and S/C ratios fixed according to the photos (Marinos and Hoek 2001) are determined. The results of these applications are going to be discussed in this study.

### General geologic setting

The peripheral foreland basin in and around the Kahramanmaraş province evolved as a result of the continental collision of the Arabian Plate and Anatolide–Taurides Platform at the beginning of the Early Miocene (Önalın 1988; Gül, et al. 2011). The northwestern basin margin is formed by the Andırın group (Triassic–Upper Cretaceous) including milky brown limestone and dolomites (Fig. 1). The main part of examined region is covered by the Karataş Formation (Lower–Middle Miocene). It contains three types of deposits, namely debris flow deposits (around the Fırın Village), mostly sandstone–lesser extent claystone alternations (north and northwest of the study area), and mostly claystone–lesser extent sandstone alternations (south and southwest of the study area). The Güredin Formation (Middle–Upper Miocene) crops out in the south of the study area. It consists of debris flow deposits (NE Kahramanmaraş Basin) and channelized conglomerates and sandstone of the Alikayası Canyon (east of the study area). The Güredin Formation contains sandstone and claystone alternation with varying ratios in the southeast of the study area (Fig. 1).

The Karataş Formation deposited in front of the slope and abyssal plains (Kozlu 1997). Sedimentary facies change of this formation might source from the irregular basin floor, distance from the main feeders' channels and the basin margin, and sedimentary process (downslope variation, sediment type, sediment quantity, etc.; Aiken et al. 2003). Conglomerate, clayey debris flows and thick-bedded sandstones evolved depending on faulting and sediment input. The finer and clay dominated sediment deposited in the quieter and deeper environmental condition (Aiken et al. 2003).

The Alikayası Canyon (Fig. 1; giant submarine canyon transported sediment from northwest) highly controlled the different sedimentary facies evolution at the end and edges of the canyon (south and southwest of the study area; Derman 1999; Gül et al. 2012b).

### Materials and methods

The geological and geotechnical data of slopes of the highway excavation (in Miocene sandstone and claystone alternations) are researched in this study. For this purpose, lithological properties' descriptions have been made and samplings collected with a total of 49 slope excavations in between the Kahramanmaraş city center and Suçatı district (Fig. 2). The thicknesses of sandstone and claystone layers were measured bed by bed to determine the relative proportions of sandstone and claystone (Fig. 3). The bedding thicknesses of sandstone are very thin. They have many discontinuity surfaces. Thus, the sandstones are slicing during the core sampling in the laboratory. Thus, the sample with standard size specified by the ASTM (2001) and ISRM (2007) used for determining the uniaxial compressive strength have not been supplied. Therefore, the block punch strength index (BPI) test, which were proposed by Ulusay et al. (2001) and adopted by the standards, is used during this study. The sandstone core samples with 1-cm thickness and 54-mm diameter had been prepared for the BPI test, then the uniaxial compressive strengths of the sandstone were determined. Moreover, fold, fault planes, discontinuity planes, discontinuity surface conditions, and unusual sandstone or claystone distributions were determined for GSI classification based on the Marinos and Hoek (2001) assumptions.

The Hoek–Brown failure criteria are used for determining the rock mass strength and deformation properties (Hoek and Brown 1980, 1997; Hoek et al. 1995, 1998, 2002; Marinos and Hoek 2001; Sönmez and Ulusay 2002; Hoek and Diederichs 2006; Asrari et al. 2014). Three parameters are taken into consideration during the Hoek–Brown failure criteria evaluations, namely the uniaxial compressive strength of solid rock ( $\sigma_{ci}$ ), Hoek–Brown constant value ( $m_i$ ), and the geological strength index (GSI). The determination of these parameters required some limitations and assumptions that are provided in following section separately for each parameter.

#### Uniaxial compressive strength $\sigma_{ci}$

“Rock strength, particularly of the uniaxial compressive strength (UCS), is an important parameter in the rock mass classification methods and approaches in various rock engineering designs (Ulusay et al. 2001).” However, the rock discontinuity, thin-layering, and schistosity structure prevent core obtaining according to the standard dimension (ASTM

**Fig. 2** Measurement locations and determined rock class of the study area. B class representing  $1 < S/C \leq 10$ ,  $GSI > 40$ , C class representing  $S/C = 1$ ,  $35 \leq GSI \leq 40$ , D–E group representing  $1/10 \leq S/C < 1$ ,  $GSI < 35$

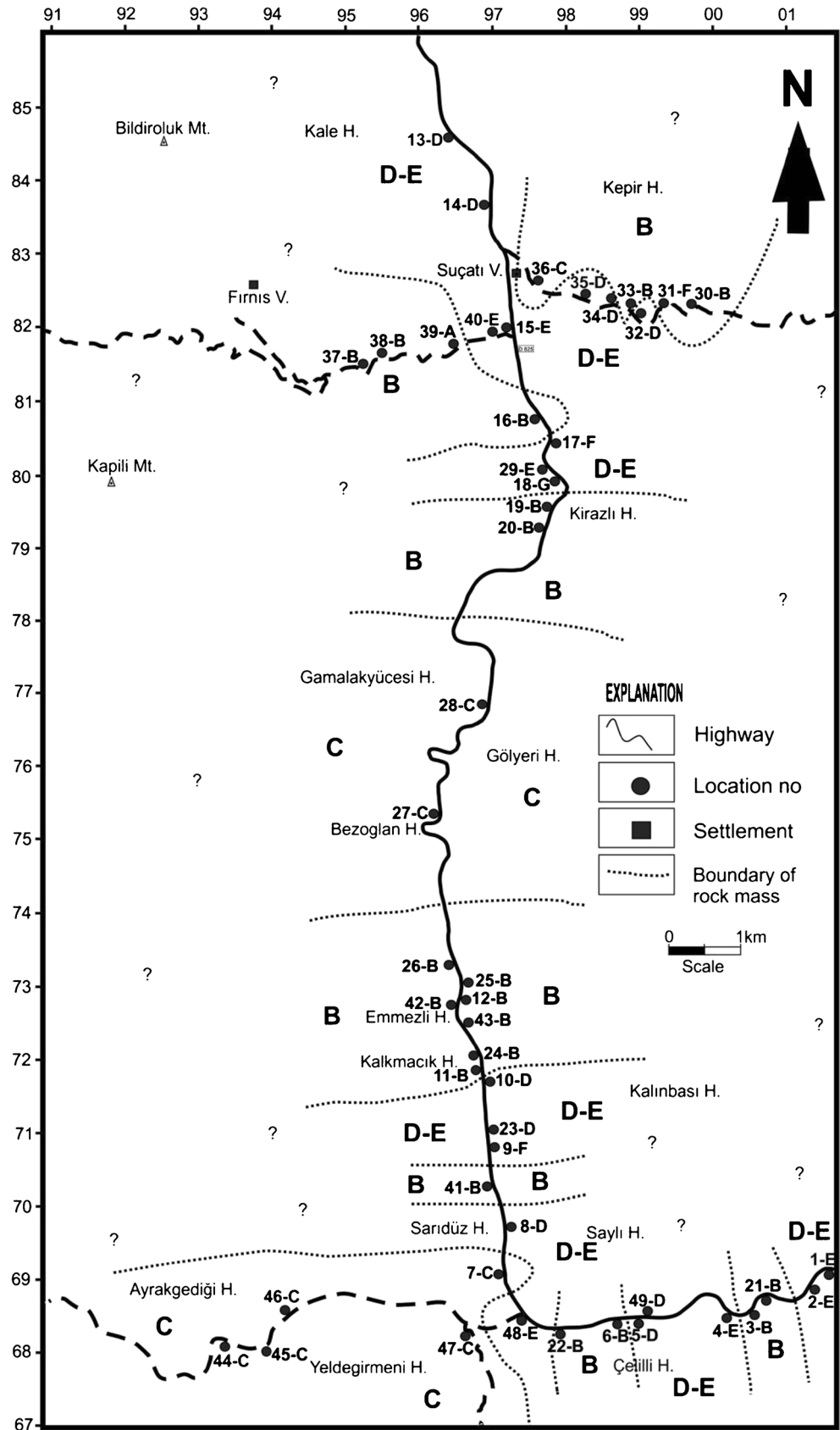


**Fig. 3** Field view of the rock mass class. **a** ‘A’ class rock at L39, **b** ‘B’ class rock at L21, **c** ‘C’ class rock at L47, **d** ‘D’ class rock at L23, **e** ‘E’ class rock at L15, **f** tectonically deformed ‘F’ class rock at L31, **g** ‘G’ class rock at L18, **h** mixed group including at least two different rock class L34; the lower part rock class is ‘E’ class, while the upper part is classified as a ‘B’ class. (Man for a scale 1.75 m)



2001; ISRM 2007). Thus, the uniaxial compressive strength is determined by indirect method. The Schmidt Hammer test, point load strength index, and block punch strength index (BPI) are widespread indirect methods.

The deep-sea sedimentary process and other controlling factors caused the deposition of laminated, thin- to medium-

bedded claystone and sandstone alternations in a large part of the Kahramanmaraş Basin during the Miocene. In the field studies, it is observed that bedding planes of alternations act as the main discontinuity planes. Moreover, the structural evolution of the units led to the development of the joint systems and tilting of beds. Those dense discontinuities prevent the

reception of the cores with desired size according to the standards. Similar situations have been previously reported by Marinos and Hoek (2001).

In this study, block punch strength index ( $BPI_c$ ) test (Ulusay et al. 2001) was used.  $BPI_c$  value, which is one of the parameters used in the rock mass classification (Table 1; Sulukcu and Ulusay 2001), can be obtained from Eq. 1. Then, uniaxial compressive strength values of sandstone samples can be indirectly determined by using Eq. 2.

$$BPI_c = 3499D^{-1.3926}t^{-1.1265}F_{t,D} \quad (1)$$

Where  $F_{t,D}$  is the failure load,  $D$  is the diameter (mm), and  $t$  is the thickness of disc specimen (mm),

$$UCS(MPa)(s_{ci}) = 5.1 * BPI_c \quad (2)$$

The uniaxial compressive strength values ( $\sigma_{ci}$ ) of the sandstone, sandstone and claystone alternations have been indirectly determined from the  $BPI_c$  value of core by using the equations proposed by the Ulusay et al. (2001). However, uniaxial compressive strength values ( $\sigma_{ci}$ ) of the complete claystone unit have been determined by using the available tables proposed by the Marinos and Hoek (2001) depending on field observations. This practice was applied only in one location (L18) in this study.

The frictional characteristics of the intact rock sample have a significant influence on the rock strength (Marinos and Hoek 2001). The constant values for all rock groups, which are proposed by Marinos and Hoek (2001), were presented in tables (Tables 2–8). The sandstone constant value is ‘17’ according to the table. The constant value of L18 is ‘6’ due to entire claystone content. Then, these constant values are used in equations.

#### Geological strength index, GSI

Although many methods have been suggested (RMR, Q, RQD, RSR, etc.) for identification and classification of rock masses and the rock mass properties, there is no separate classification that has been proposed for heterogeneous rocks. Firstly, Hoek et al. (1995) and Hoek and Brown (1997) have included GSI instead of RMR for the prediction

of rock mass properties. Then, Marinos and Hoek (2001) adopted GSI to the study of flysch-type heterogeneous rocks, and they have proposed a separate classification table (Table 2).

Marinos and Hoek (2001) presented eight representative field photos of the rocks belonging to the different lithology, which can be used for determining the GSI values of the heterogeneous sandstone–claystone-type rocks. The sandstone/claystone rates (S/C) (recommended by the Budetta and Nappi (2011)) are used in this study for quantitative description. However, the class intervals of Budetta and Nappi (2011) classifications have been partly changed. Additional sandstone/claystone ratios have been proposed and presented in Table 3 according to the field photos of Marinos and Hoek (2001). Detail GSI' values have been fixed based on the information in Table 2. During the determination of these values, sandstone/claystone ratio, discontinuity surface conditions, and favorable or unfavorable bed inclination according to excavation slopes were taken into consideration.

#### Estimation of $\sigma_{ci}$ and $m_i$ for heterogeneous sandstone and claystone alternation

Marinos and Hoek (2001) pointed out that laboratory or field test results of the claystones and sandstones cannot be directly used to determine  $\sigma_{ci}$  and  $m_i$ , parameters of heterogeneous rocks. Instead of this, an average value representing both units should be used. They also suggested that if the field contains a heterogeneous unit with hundreds bedding surfaces (similar to our study area), the  $\sigma_{ci}$  and  $m_i$  parameters of sandstone and claystone alternations should be lower than the tough sandstone bed values. The decreasing ratio is fixed based on sandstone/claystone (S/C) ratios, faulting and folding (Table 4) and applied to tough sandstone values. Consequently, resultant parameters are determined for heterogeneous alternations.

ROCLAB free software (Rockscience inc. 2002) used for determining the tensile strength ( $\sigma_t$ ), uniaxial compressive strength ( $\sigma_c$ ), the global strength ( $\sigma_{cm}$ ), deformation modulus ( $E_m$ ), the Hoek–Brown rock masses constant ( $m_b$ ), constants ( $s$  and  $a$ ) depending on the characteristics of the rock mass, Mohr–Coulomb's criteria cohesion ( $c'$ ), and friction angle ( $\phi$ ) values from heterogeneous rock mass parameters.

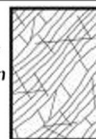
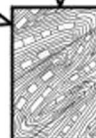
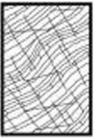
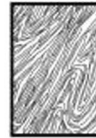
## Results and discussions

The conglomerate, sandstone, and claystone units with different proportions in the north of the Kahramanmaraş Province are classified under the different sedimentary facies. The sandstone and conglomerate (more resistant units in terms of engineering geology) are mainly observed to the north of Kahramanmaraş. The region located in the northwest of

**Table 1** Classification of block punch strength index (Sulukcu and Ulusay 2001)

$BPI_c$	Strength class
<1	Very weak
1–5	Weak
5–10	Moderate
10–20	Medium
20–50	High
>50	Very high

**Table 2** GSI estimates for heterogeneous rock masses such as flysch (Marinos and Hoek 2001)

GSI FOR HETEROGENEOUS ROCK MASSES SUCH AS FLYSCH (Marinos P and Hoek E, 2000)		SURFACE CONDITIONS OF DISCONTINUITIES (Predominantly bedding planes)				
From a description of the lithology, structure and surface conditions (particularly of the bedding planes), choose a box in the chart. Locate the position in the box that corresponds to the condition of the discontinuities and estimate the average value of GSI from the contours. Do not attempt to be too precise. Quoting a range from 33 to 37 is more realistic than giving GSI = 35. Note that the Hoek-Brown criterion does not apply to structurally controlled failures. Where unfavourably oriented continuous weak planar discontinuities are present, these will dominate the behaviour of the rock mass. The strength of some rock masses is reduced by the presence of groundwater and this can be allowed for by a slight shift to the right in the columns for fair, poor and very poor conditions. Water pressure does not change the value of GSI and it is dealt with by using effective stress analysis.		VERY GOOD - Very rough, fresh unweathered surfaces	GOOD - Rough, slightly weathered surfaces	FAIR - Smooth, moderately weathered and altered surfaces	POOR - Very smooth, occasionally slickensided surfaces with compact coatings or fillings with angular fragments	VERY POOR - Very smooth slickensided or highly weathered surfaces with soft clay coatings or fillings
COMPOSITION AND STRUCTURE						
	<b>A. Thick bedded, very blocky sandstone</b> The effect of pelitic coatings on the bedding planes is minimized by the confinement of the rock mass. In shallow tunnels or slopes these bedding planes may cause structurally controlled instability.	70	60	A		
	<b>B. Sandstone with thin inter-layers of siltstone</b>		50	B	C	D
	<b>C. Sandstone and siltstone in similar amounts</b>					
	<b>D. Siltstone or silty shale with sandstone layers</b>					
	<b>E. Weak siltstone or clayey shale with sandstone layers</b>		40			
C, D, E and G - may be more or less folded than illustrated but this does not change the strength. Tectonic deformation, faulting and loss of continuity moves these categories to F and H.					30	
	<b>F. Tectonically deformed, intensively folded/faulted, sheared clayey shale or siltstone with broken and deformed sandstone layers forming an almost chaotic structure</b>					20
	<b>G. Undisturbed silty or clayey shale with or without a few very thin sandstone layers</b>				G	
	<b>H. Tectonically deformed silty or clayey shale forming a chaotic structure with pockets of clay. Thin layers of sandstone are transformed into small rock pieces.</b>					H 10

→ : Means deformation after tectonic disturbance

Kahramanmaraş contains mainly claystone having a lower resistance in terms of engineering geology. Different types of mass movements (sliding, flowing, falling, etc.) may occur in slope excavation, depending on unfavorable bed inclinations, surface weathering, orientation and alignment of discontinuity surfaces, and rainfall.

**Table 3** Sandstone/claystone ratio for class of heterogeneous rock masses

Rock mass class	Sandstone (S)/claystone (C)
A	>10
B	1 < S/C ≤ 10
C	1
D	1/3 ≤ S/C < 1
E	1/10 ≤ S/C < 1/3
F	Tectonically deformed claystone with sandstone
G	< 1/10
H	Tectonically deformed claystone

This study contains information obtained from the forty-nine excavation slopes with varying thickness opened on the main road of the Kahramanmaraş–Göksun and secondary

**Table 4** Suggested proportions of parameters  $\sigma_{ci}$  and  $m_i$  for estimating rock mass properties for Flysch (Marinos and Hoek 2001)

Flysch type,	Proportions of values for each rock type to be included in rock mass property determination
A and B	Use values for sandstone beds
C	Reduce sandstone values by 20 % and use full values for siltstone
D	Reduce sandstone values by 40 % and use full values for siltstone
E	Reduce sandstone values by 40 % and use full values for siltstone
F	Reduce sandstone values by 60 % and use full values for siltstone
G	Use values for siltstone or shale
H	Use values for siltstone or shale

roads to the Andirın town and Ilca town (Fig. 2). The block punch strength index test performed on sandstone samples taken from slope, and  $\sigma_{ci}$  have been determined. The constant  $m_i$  value is '17' for 48 location, while it is a '6' for L18 including completely claystone. Marinós and Hoek (2001) offered that the  $\sigma_{ci}$  and constant  $m_i$  values are decreased according to ratios specified in Tables 2 and 3 due to heterogeneous rock mass properties (Table 4). Revised values of  $\sigma_{ci}$  and constant  $m_i$  values are presented in Table 5.

The  $BPI_c$  ranges from 4.72 to 12.09 MPa. The studied rocks can be classified as “weak strength” in two locations (L6, L7); “medium strength” in five locations (L17, 24, 25, 27, 29); and “moderate strength” in another 42 locations according to Sulukcu and Ulusay (2001) classification. The revised  $\sigma_{ci}$  values range from 13.61 to 55.54 MPa, while revised constant  $m_i$  values range from 6 to 17 (Table 5).  $\sigma_{ci}$  value of L18 is 13 MPa. During the determination of this value, the hardly separated claystone lamina by pocket knife and lowest sandstone–claystone alternation strength (13.61 MPa) was taken into account. The GSI values are defined based on Tables 2 and 3; the intact modulus ( $E_i$ ), sandstone/claystone ratio, and rock mass classes are presented in Table 6.

The uniform, parallel bedded sandstone and claystone alternations with different proportions are shown in Fig. 3a–e. Figure 3f is the field photos of the sandstone/claystone alternations with a ratio corresponding to the ‘B’ class, while it is classified as the ‘F’ class due to reverse faulted and folded properties. Tectonic effects (developed after the Miocene) led to the formation of large-scale basin margin faults and small-scale faults and folds in the Kahramanmaraş Basin interior (Önalán 1988; Robertson et al. 2004; Gül et al. 2012b). The sedimentary process during the basin evolution led to the deposition of the fining–thinning upward and downward slope sequences through the deeper basin interior (Gül 2004). These sedimentary processes, sediment type, sediment input location, and basin floor irregularity can lead to rock mass with different classes and a mixed group (including at least two different rock mass) close to source-basin margin (Fig. 3h) and entirely claystones in the deepest part of the basin (Fig. 3g). The mixed group may contain coarse-grained (‘A, B, and C’ classes) and fine-grained part (‘D, E, and G’ classes) with limited thickness. The mixed groups are classified based on total sandstone and claystone bed thickness ratio. However, during the engineering application, each rock mass may behave in different characters. For example, surface between the thick sandstone and thick claystone acts as a main failure surface.

Three different rock classes, the ‘B, C, and D–E’ classes were mapped on the basis of rock mass class marked on the location map (Fig. 3). The boundaries of those groups cannot be determined outside the rock excavation slopes due to surface weathering and dense vegetation. The ‘B’ class rocks

**Table 5** Corrected  $\sigma_{ci}$  (obtained from  $BPI_c$  values) and  $m_i$  parameters

Location no.	$BPI_c$ (MPa)	$\sigma_{ci}$ (MPa)	Corrected $\sigma_{ci}$ (MPa)	Constant $m_i$	Corrected constant $m_i$
L-1	6.96	35.50	21.30	17.00	10.20
L-2	6.99	35.65	21.39	17.00	10.20
L-3	6.20	31.62	31.62	17.00	17.00
L-4	6.48	33.05	19.83	17.00	10.20
L-5	7.23	36.87	22.12	17.00	10.20
L-6	4.95	25.25	25.25	17.00	17.00
L-7	4.72	24.07	19.26	17.00	13.60
L-8	6.82	34.78	20.87	17.00	10.20
L-9	7.30	37.23	14.89	17.00	6.80
L-10	6.76	34.48	20.69	17.00	10.20
L-11	5.70	29.07	29.07	17.00	17.00
L-12	8.60	43.86	43.86	17.00	17.00
L-13	6.30	32.13	19.28	17.00	10.20
L-14	5.95	30.35	18.21	17.00	10.20
L-15	5.66	28.87	17.32	17.00	10.20
L-16	7.93	40.44	40.44	17.00	17.00
L-17	10.70	54.57	21.83	17.00	6.80
<sup>a</sup> L-18	–	13.00	13.00	6.00	6.00
L-19	9.21	46.97	46.97	17.00	17.00
L-20	5.04	25.70	25.70	17.00	17.00
L-21	6.02	30.70	30.70	17.00	17.00
L-22	7.68	39.17	31.33	17.00	13.60
L-23	7.24	36.92	22.15	17.00	10.20
L-24	10.89	55.54	55.54	17.00	17.00
L-25	10.53	53.70	53.70	17.00	17.00
L-26	7.60	38.76	38.76	17.00	17.00
L-27	12.09	61.66	49.33	17.00	13.60
L-28	8.85	45.14	36.11	17.00	13.60
L-29	10.44	53.24	31.95	17.00	10.20
L-30	6.70	34.17	34.17	17.00	17.00
L-31	6.67	34.02	13.61	17.00	6.80
L-32	9.22	47.02	28.21	17.00	10.20
L-33	5.84	29.78	29.78	17.00	17.00
L-34	5.91	30.14	18.08	17.00	10.20
L-35	6.10	31.11	18.67	17.00	10.20
L-36	5.60	28.56	22.85	17.00	13.60
L-37	5.84	29.78	29.78	17.00	17.00
L-38	7.59	38.71	38.71	17.00	17.00
L-39	7.35	37.49	37.49	17.00	17.00
L-40	5.50	28.05	16.83	17.00	10.20
L-41	6.79	34.63	34.63	17.00	17.00
L-42	7.09	36.16	36.16	17.00	17.00
L-43	5.75	29.33	29.33	17.00	17.00
L-44	8.20	41.82	33.46	17.00	13.60
L-45	7.39	37.69	30.15	17.00	13.60
L-46	7.31	37.28	29.82	17.00	13.60
L-47	7.97	40.65	32.52	17.00	13.60
L-48	6.35	32.39	19.43	17.00	10.20
L-49	6.95	35.45	21.27	17.00	10.20

<sup>a</sup> This uniaxial compressive strength of intact rock estimated according to field observation based on Marinós and Hoek (2001) suggestion

**Table 6** Detailed rock mass data sandstone/claystone ratio (S/C), (geological strength index) GSI and intact modulus ( $E_i$ )

Location No	$E_i$ (Mpa)	S/C	Rock mass class	GSI
L-1	5,538.00	0.29	E <sup>a</sup>	29
L-2	5,561.40	0.20	E	26
L-3	8,221.20	3.33	B	45
L-4	5,155.80	0.30	E <sup>a</sup>	30
L-5	5,751.20	0.50	D	35
L-6	6,565.00	1.50	B	42
L-7	5,007.60	1.00	C	38
L-8	5,426.20	0.40	D	35
L-9	3,871.40	0.50	F	20
L-10	5,379.40	0.60	D	35
L-11	7,558.20	4.00	B	43
L-12	11,403.60	3.50	B	46
L-13	5,012.80	0.60	D	32
L-14	4,734.60	0.80	D	33
L-15	4,503.20	0.25	E	28
L-16	10,514.40	3.00	B	45
L-17	5,675.80	0.60	F	20
L-18	3,250.00	0.05	G	22
L-19	12,212.20	5.00	B	48
L-20	6,682.00	5.70	B	42
L-21	7,870.20	4.00	B	48
L-22	8,145.80	1.50	B	42
L-23	5,759.00	0.35	D	33
L-24	14,440.40	4.00	B	47
L-25	13,962.00	2.00	B	45
L-26	10,077.60	2.20	B	43
L-27	12,825.80	1.00	C	40
L-28	9,388.60	1.00	C	37
L-29	8,307.00	0.25	E	28
L-30	8,884.20	1.50	B	45
L-31	3,538.60	2.20	F	23
L-32	7,334.60	0.70	D	33
L-33	7,742.80	3.00	B	45
L-34	4,700.80	0.66	D <sup>a</sup>	32
L-35	4,854.20	0.50	D	35
L-36	5,941.00	1.00	C	37
L-37	7,742.80	1.50	B	42
L-38	10,064.60	5.60	B	48
L-39	9,747.40	14.00	A	55
L-40	4,375.80	0.20	E	26
L-41	9,003.80	6.00	B	47
L-42	9,401.60	2.00	B <sup>a</sup>	45
L-43	7,625.80	1.50	B	45
L-44	8,699.60	1.00	C	38
L-45	7,839.00	1.00	C	37
L-46	7,753.20	1.00	C	36
L-47	8,455.20	1.00	C	37
L-48	5,051.80	0.25	E <sup>a</sup>	28
L-49	5,530.20	0.40	D	35

<sup>a</sup> Mixed group including at least two different rock classes. Presented rock class proposed according to sandstone and claystone ratio

have been largely identified in the northern part of the study area, due to the proximity of the basin margin and the presence of channels (transported coarse-grained sediment into the basin). The fine-grained, relatively low-strength sandstone and claystone alternations ('D–E' class) crop out around the coarse-grained units. The coarse-grained (mainly sandstone) units crop out in the central part of study area ('B and C' classes). This area is located between the basin margin (west) and the Alikayası Canyon (east). The 'C' class rock mass crops out in the SW of the study area. The 'B and D–E' classes rock mass are intercalated in the southeast of the study area, just in front of the Alikayası Canyon ending. The coarse-grained sediment and debris flow deposits crop out around the canyon (Derman 1999; Aiken et al. 2003). The 'B' class rock mass evolved depending on coarse-grained sediment transport, while subsequent quiet environmental condition led to the deposition of the 'D–E' classes of rock mass.

Gül et al. (2012a) presented an analysis of Landsat images of the Kahramanmaraş Basin. It contains a colorful image depending on light reflectance differentiation due to lithological properties, vegetation, water content, and mineralogical content of the geologic units. The color variations of the Karataş and Güredin Formation satellite image give similar distributions with the rock mass class determined in this study. Therefore, Landsat satellite images could be used in determining the covered rock mass types of the heterogeneous rocks.

The rock mass of the Kahramanmaraş Basin have been divided into four different groups (Table 7) based on the GSI values and the rock mass group determined based on S/C ratio. (1) The 'A–B' classes have the highest S/C ratio (S/C >1) and the highest GSI (GIS>40) and are forming the 40 % of the study area. (2) The 'C' class (S/C=1) has a relatively higher GSI (35≤GIS≤40) and is forming the 16 % of the study area. (3) The 'D–E' classes have the lower S/C ratio (1>S/C>1/10) and lower GSI (25≤GIS<35) and are forming the 35 % of the study area. (4) The 'F–G' classes have the lowest S/C ratio (S/C <1/10) and lowest GSI (<25) and are forming the small part of study area (8 %). The 'F' class rock mass contains tectonically deformed strata. The G class rock masses contain entirely claystone.

As a result of the field observations and laboratory data, the deep-sea sediments of the Kahramanmaraş have been divided into six classes according to the S/C ratio and four classes

**Table 7** GSI values of the rock mass class

Rock mass class	GSI	Percentage of rock mass based on the GSI values
A–B	>40	41
C	40–35	16
D–E	25–34	35
F–G	<25	8

based on the values of GSI. However, Budetta and Nappi (2011) have separated four different classes according to S/C ratio and three classes based on GSI value in the San Mauro formation, which has similar lithological units with the Kahramanmaraş Basin. The S/C ratio of different classes proposed by Budetta and Nappi (2011) are  $S/C > 2$  for the 'A' class,  $S/C$  between 1 and 2 for the 'B' class,  $S/C = 1$  for the 'C' class, and  $S/C < 1$  for the 'D' class. The S/C ratio have re-described based on original pictures (see Fig. 3 of Marinos and Hoek (2001)), and six different classes have been determined (Table 3) within this study. The S/C ratios of the studied 49 locations (results of direct measurements during the field study) have evaluated based on this new proposal. The separation of sandstone and claystone is one of the most fundamental issues of geology education. By this way, the engineers, working on the heterogeneous flysch rocks, can easily determine the S/C ratio and rock class and then they will determine much more accurately and easily Hoek–Brown criteria values based on the S/C ratio and discontinuity surface condition.

The rock mass strength parameters based on the Hoek–Brown or Mohr–Coulomb criteria were calculated using the ROCLAB Free software (Rockscience inc. 2002) for the general case (Table 5). The slopes of the study area are mechanically excavated; thus, the disturbance factor ( $D$ ) is taken as 0.7 in the calculations. The intact modulus ( $E_i$ ) value of the units in the study area are calculated based on the Hoek and Diederichs (2006) assumptions by using the modulus ratio (MR) and  $\sigma_{ci}$  in Eq. 3.

$$E_i = MR \cdot \sigma_{ci} \quad (3)$$

The cohesion values ( $c'$ ) vary between 0.16 and 2.18 MPa, internal friction angle ( $\phi$ ) changes between  $9.72^\circ$  and  $29.25^\circ$ , and modulus of elasticity ( $E_m$ ) between 90.39 and 1,439.16 MPa (Table 8). If the strength parameters of the 49 locations are taken into consideration, the lowest  $c'$ ,  $\phi$ , and  $E_m$  have been obtained from the 'E and D' rock classes. The strength parameters are increasing depending on the sandstone ratio increasing (without rocks of tectonically deformed rocks) in rocky bodies of the 'A and B' classes.

A circular type of failure defined in heterogeneous rock by Mandrone (2006) is not observed in our field. The bedding planes of the sandstones and claystones of the study area act as main discontinuity surfaces during the slope excavation. Especially, if the slope excavations (for example road cut) opened in the direction perpendicular to the inclination of bedding, planar-type failure evolves depending on joint crossing with bedding surfaces. Observations and measurements on the road cuts in the study area indicate the lack of potential for a large mass movement; therefore, the Hoek–Brown failure criteria are applied to the general case. Wedge-type failure was observed in the claystone rather than planar failure. An

intersection of the small shear surfaces causes wedge formation. The fragments in a size of 0.1–5 cm have evolved as a result of this type failure and accumulated in front of the slopes (Figs. 3d, f, h). Similar to the Budetta and Nappi (2011) approach, the region has a high S/C ratio in our study area and is more stable, while the region carrying a higher risk of landslides has a lower S/C ratio and is tectonically deformed.

Marinos and Hoek (2001), Mandrone (2006), and Budetta and Nappi (2011) emphasized that the heterogeneity of rocks caused stability problems. Marinos and Hoek (2001) method's success largely depends on knowledge, experience, and observational assessments of the engineers. Budetta and Nappi (2011) proposed the sandstone/claystone rates for a few rock class presented in Marinos and Hoek (2001). This study is offered sandstone and claystone ratio for all rock masses seen in the field photos of the Marinos and Hoek (2001) study. Rates of sandstone and claystone can be easily measured in the field with the bed thickness. After that, S/C ratio is calculated and rock mass properties of each group can be calculated or estimated by using the necessary equations or charts. In the meantime, depending on sedimentary facies change of deep-sea sediments, a different rock mass class could be found in the same slope that caused mixed class development.

## Conclusion

The sedimentary processes, sediment basin entry points, sediment type, sediment transport distance, and varied topography of the basin floor of the Kahramanmaraş Basin during the Miocene time led to the deposition of conglomerate, largely sandstone, and claystone in variable proportions.

The Hoek–Brown constant value is 17 for 48 locations and is six for one location (L18, including completely claystone).  $\sigma_{ci}$  values were indirectly fixed with block punch strength index test. The heterogeneous rock mass (sandstone and claystone alternation) strength is lower than the pure sandstone strength due to clay content. Thus, decreasing the ratio applied to  $\sigma_{ci}$  values are obtained from sandstone depending on heterogeneity. The revised  $\sigma_{ci}$  values vary between 13.61 and 55.54 MPa. The rock masses of the study area are divided into seven classes based on S/C ratio and tectonic deformation according to the Marinos and Hoek (2001) method. According to these groups and GSI values (fixed based on discontinuity surface condition), four different groups are fixed. The 'B, C, and D–E' rock masses are separately mapped depending on rock mass distributions of each location. Planar-type failure may be observed in the sandstone rich—the 'B and C' rock classes'—area. They are found close to

**Table 8** Hoek–Brown classification constants ( $m_b$ ,  $s$ , and  $a$ ), the Mohr–Coulomb parameters ( $c'$  and  $\phi'$ ) and rock mass parameters of examined locations

Location no.	Hoek–Brown criteria			Mohr–Coulomb fit		Rock mass parameters			
	$m_b$	$s*(10^{-4})$	$a$	$c'$ (Mpa)	$\phi'$ (°)	$\sigma_t$ (MPa)* ( $10^{-2}$ )	$\sigma_c$ (MPa)	$\sigma_{cm}$ (MPa)	$E_m$ (MPa)
L-1	0.19	0.25	0.53	0.40	14.16	-0.30	0.08	1.03	178.46
L-2	0.20	0.29	0.53	0.42	14.52	-0.30	0.09	1.08	185.55
L-3	0.83	3.00	0.51	1.19	24.82	-1.30	0.55	3.72	643.38
L-4	0.19	0.25	0.53	0.38	14.16	-0.30	0.08	0.96	166.14
L-5	0.29	1.00	0.52	0.54	17.10	-0.60	0.17	1.45	257.65
L-6	0.63	2.00	0.51	0.84	22.68	-0.70	0.30	2.53	382.28
L-7	0.45	1.00	0.51	0.56	20.22	-0.50	0.19	1.62	261.34
L-8	0.29	1.00	0.52	0.50	17.10	-0.60	0.16	1.37	243.09
L-9	0.08	0.09	0.54	0.18	9.72	-0.20	0.03	0.42	102.70
L-10	0.29	1.00	0.52	0.50	17.10	-0.60	0.16	1.35	240.99
L-11	0.74	3.00	0.51	1.04	23.96	-1.00	0.43	3.21	523.84
L-12	0.88	4.00	0.51	1.69	25.26	-2.00	0.83	5.32	949.50
L-13	0.24	1.00	0.52	0.43	15.98	-0.40	0.12	1.13	195.76
L-14	0.26	1.00	0.52	0.42	16.35	-0.40	0.12	1.11	193.21
L-15	0.18	0.22	0.53	0.32	13.80	-0.20	0.06	0.81	140.41
L-16	0.83	3.00	0.51	1.52	24.82	-1.70	0.71	4.75	822.84
L-17	0.08	0.09	0.54	0.26	9.72	-0.20	0.04	0.62	150.56
L-18	0.08	0.12	0.54	0.16	9.79	-0.20	0.03	0.38	90.39
L-19	0.98	5.00	0.51	1.89	26.13	-2.60	1.03	6.06	1,153.24
L-20	0.70	2.00	0.51	0.90	23.53	-0.80	0.35	2.75	436.48
L-21	0.98	5.00	0.51	1.22	26.13	-1.70	0.67	3.90	743.21
L-22	0.50	2.00	0.51	0.96	21.03	-1.00	0.37	2.81	474.33
L-23	0.26	1.00	0.52	0.51	16.35	-0.50	0.14	1.35	235.01
L-24	0.92	5.00	0.51	2.18	25.69	-2.80	1.13	6.94	1,280.11
L-25	0.83	3.00	0.51	2.02	24.82	-2.20	0.94	6.31	1,092.64
L-26	0.74	3.00	0.51	1.39	23.96	-1.40	0.58	4.28	698.46
L-27	0.50	2.00	0.51	1.52	21.03	-1.60	0.58	4.42	746.85
L-28	0.43	1.00	0.51	1.03	19.81	-0.90	0.33	2.93	464.92
L-29	0.17	0.19	0.53	0.56	13.44	-0.40	0.10	1.43	251.07
L-30	0.83	3.00	0.51	1.28	24.82	-1.40	0.60	4.02	695.26
L-31	0.10	0.14	0.54	0.19	10.67	-0.20	0.03	0.45	101.02
L-32	0.26	1.00	0.52	0.64	16.35	-0.70	0.18	1.72	299.31
L-33	0.83	3.00	0.51	1.12	24.82	-1.20	0.52	3.50	605.94
L-34	0.24	1.00	0.52	0.40	15.98	-0.40	0.11	1.06	183.58
L-35	0.29	1.00	0.52	0.45	17.10	-0.50	0.15	1.22	217.46
L-36	0.43	1.00	0.51	0.65	19.81	-0.60	0.21	1.86	294.19
L-37	0.63	2.00	0.51	1.00	22.68	-0.80	0.35	2.99	450.87
L-38	0.98	5.00	0.51	1.56	26.13	-2.10	0.85	4.99	950.43
L-39	1.43	15.00	0.50	1.75	29.25	-3.80	1.40	5.97	1,439.16
L-40	0.18	0.22	0.53	0.31	13.80	-0.20	0.06	0.78	136.44
L-41	0.92	5.00	0.51	1.36	25.69	-1.70	0.71	4.33	798.17
L-42	0.83	3.00	0.51	1.36	24.82	-1.50	0.63	4.25	735.75
L-43	0.83	3.00	0.51	1.10	24.82	-1.20	0.51	3.45	596.78
L-44	0.45	1.00	0.51	0.98	20.22	-0.90	0.33	2.81	454.03
L-45	0.43	1.00	0.51	0.86	19.81	-0.80	0.28	2.45	388.18
L-46	0.40	1.00	0.52	0.83	19.41	-0.70	0.25	2.34	364.87
L-47	0.43	1.00	0.51	0.93	19.81	-0.80	0.30	2.64	418.69
L-48	0.20	0.29	0.53	0.38	14.52	-0.30	0.08	0.98	168.55
L-49	0.29	1.00	0.52	0.51	17.10	-0.6	0.17	1.39	247.75

\* $c'$  effective cohesion

coarse-grained sediment source such as basin margin or canyon. Small wedge-type failure can be observed in the fine-grained section of the ‘D–E’ rock classes.

The Marinós and Hoek (2001) method’s success are depending on the good understanding of the definition, successful implementation of the method, having enough knowledge and experience of engineers, and availability outcrop area. This study proposes the more qualitative study on the differentiation of rock classes based on S/C ratio.

**Acknowledgments** The authors thank Mr. Feridun Öncel, Mr. Hasan Aksoy, and Mr. Ferhat Aydın for their contribution during the field and laboratory studies. The authors warmly thank the anonymous reviewer and Editor Prof. Dr. Biswajeet Pradhan for their valuable contributions.

## References

- Agan C (2014) Engineering geological and geomechanical assessments of the proposed Mezra dam site (Şanlıurfa, Turkey). *Arab J Geosci*. doi:10.1007/s12517-014-1317-y
- Aiken E, Cronin BT, Gürbüz K, Gül M (2003) Maraş Foreland Basin in Southern Turkey: two examples of downslope characteristics from re-sedimentation processes in deep-water. *Submarine Slope Systems, Processes, Products & Prediction Conference*, Liverpool, England, pp 15
- Alemdag S (2014) Assessment of bearing capacity and permeability of foundation rocks at the Gumustas waste dam site (NE Turkey) using empirical and numerical analysis. *Arab J Geosci*. doi:10.1007/s12517-013-1236-3
- Amit Verma K, Singh TN (2010) Assessment of tunnel instability—a numerical approach. *Arab J Geosci* 3:181–192. doi:10.1007/s12517-009-0066-9
- Asrari AA, Shahriar K, Ataeepour M (2014) The performance of ANFIS model for prediction of deformation modulus of rock mass. *Arab J Geosci*. doi:10.1007/s12517-013-1097-9
- ASTM (2001) Standard test method of unconfined compressive strength of intact rock core specimens. ASTM Stand 04.08(D2938)
- Bouma AH (2004) Key controls on the characteristics of turbidite systems. In: Lomas SA, Joseph P (eds) *Geological society*, vol 222. Special Publications, London, pp 9–23
- Budetta P, Nappi M (2011) Heterogeneous rock mass classification by means of the geological strength index: the San Mauro formation (Cilento, Italy). *Bull Eng Geol Environ* 70:585–593
- Derman AS (1999) Proximal submarine fan conglomerate and valley fill pattern. 12nd Petroleum Congress of Turkey, pp 207–218
- Gül M (2004) Evolution of the turbidite system in the Kahraman Maraş Basin. Cukurova University Institute of Basic and Applied Science, PhD Dissertation
- Gül M, Gürbüz K, Cronin BT (2011) Provenance of the northern part of the Kahramanmaraş peripheral foreland basin (Miocene, S Turkey). *J Asian Earth Sci* 40–2:475–495
- Gül M, Gürbüz K, Kalelioğlu Ö (2012a) Lithology discrimination in foreland basin with using Landsat TM images. *J Indian Remote Sens Soc* 40–2:257–269
- Gül M, Cronin BT, Gürbüz K (2012b) Confined deep water system development on the accretionary wedge (Miocene, Kahramanmaraş Foreland Basin, S Turkey). *Earth Sci Rev* 114(3–4):195–217
- Hoek E, Brown ET (1980) Empirical strength criterion for rock masses. *J. Geotech. Engng Div. ASCE*, 106 (GT9):1013–1035.
- Hoek E, Brown ET (1997) Practical estimates of rock mass strength. *Int J Rock Mech Min Sci Geomech Abstr* 34–8:1165–1186
- Hoek E, Diederichs MS (2006) Empirical estimation of rock mass modulus. *Int J Rock Mech Min Sci* 43:203–215
- Hoek E, Kaiser PK, Bawden WF (1995) *Support of underground excavations in hard rock*. Balkema, Rotterdam
- Hoek E, Marinós P, Benissi M (1998) Applicability of the geological strength index (GSI) classification for very weak and sheared rock masses. The case of the Athens Schist formation. *Bull Eng Geol Environ* 57:151–160
- Hoek E, Carranza-Torres C, Corkum B (2002) Hoek-Brown criterion—2002 edition. *Proc. NARMS-TAC Conf Tor 1*:267–273
- ISRM (2007) The complete ISRM suggested methods for rock characterization, testing and monitoring: 1974–2006. In: Ulusay R and Hudson (eds) *Suggested methods prepared by the commission on testing methods*, International Society for Rock Mechanics
- Kissel C, Laj C, Poisson A, Görür N (2003) Paleomagnetic reconstruction of the Cenozoic evolution of the Eastern Mediterranean. *Tectonophysics* 362:199–217
- Kozlu H (1997) Tectono-stratigraphic units of the Neogene basins (İskenderun, Misis–Andırın) and their evaluation in the Eastern Mediterranean region. PhD Dissertation, Cukurova University Institute of Basic and Applied Science (in Turkish, with English Abstr.).
- Ma K, Tang CA, Li LC, Ranjith PG, Cai M, Xu NW (2013) 3D modeling of stratified and irregularly jointed rock slope and its progressive failure. *Arab J Geosci* 6:2147–2163. doi:10.1007/s12517-012-0578-6
- Mandrone G (2006) Engineering geological mapping of heterogeneous rock masses in the Northern Apennines: an example from the Parma Valley (Italy). *Bull Eng Geol Environ* 65:245–252
- Marinós P, Hoek E (2001) Estimating the geotechnical properties of heterogeneous rock masses such as flysch. *Bull Eng Geol Environ* 61:85–92
- Moomivand H (2014) Effects of orientation, frequency, and number of sets of discontinuities on rock strength under triaxial stresses. *Arab J Geosci*. doi:10.1007/s12517-013-1069-0
- Önalın M (1988) Geological evolution of the Maraş Tertiary peripheral basin. *Geological Bulletin of Turkey* 29:49–63 (unpublished, in Turkish, with English Abstr.).
- Robertson AHF, Ünlügenç UC, İnan N, Taşlı K (2004) The Misis–Andırın complex: a mid-tertiary melange related to late-stage subduction of the Southern Neotethys in S Turkey. *J Asian Earth Sci* 22: 413–453
- Rockscience inc. (2002) ROCLAB Rock mass strength analysis using the generalized Hoek-Brown failure criterion, Toronto, available at <http://www.rockscience.com>
- Şen Z (2014) Rock quality designation-fracture intensity index method for geomechanical classification. *Arab J Geosci* 7:2915–2922. doi:10.1007/s12517-013-0975-5
- Sönmez H, Ulusay R (2002) A discussion on the Hoek–Brown failure criterion and suggested modifications to the criterion verified by slope stability case studies. *Yerbilimleri* 26:77–99
- Sulukcu S, Ulusay R (2001) Evaluation of the block punch index test with prime consideration on size effect, failure mechanism and its effectiveness in predicting rock strength. *Int J Rock Mech Min Sci* 38–8: 1091–1111
- Ulusay R, Gokceoglu C, Sulukcu S (2001) Draft ISRM suggested method for determining block punch strength index (BPI). *Int J Rock Mech Min Sci* 38:1113–1119
- Walker RG (1978) Deep water sandstone facies and ancient submarine fans: models for exploration for stratigraphic traps. *Bull Am Assoc Pet Geol* 62:932–966